STUDY OF TURBULENT FLOW OVER A PC-9 TRAINER WING SECTION WITH THE USE OF CFD FLOTRAN

Fokin D., Vollan A.

Chebotarev Institute of Mathematics and Mechanics (Russia),
Pilatus Aircraft Ltd, Stans CH-6470 (Switzerland)

Introduction

Modern engineering analysis can not be imagined without intensive use of computer aided technologies allowing to investigate numerically a wide range physical phenomena. CFD FLOTRAN is one of the powerful tools making possible the comprehensive investigation, design and optimization of complicated engineering objects. The present paper is devoted to the use of CFD FLOTRAN for solving particular engineering problems of the analysis of viscous turbulent flow over a PC-9 trainer middle span wing section for different flow conditions with and without a spoiler.

1. ANSYS FLOTRAN

CFD FLOTRAN is a finite element code for calculation of two and three dimensional viscous compressible unsteady and steady flows. Five independent variables p – pressure, T – temperature, u, v, w – velocity components satisfy to five equations: continuity equation, three momentum equations and the perfect gas equation. In the case of the turbulent flow CFD FLOTRAN solves the time averaged Navier-Stockes equations with the introduction of a new unknown: turbulent viscosity $\mu_t=C_\mu\rho k^2/\varepsilon$, where $C_\mu=0.09$ is an empirical constant, ρ is the flow density, k is the kinetic energy, ε is the dissipation of turbulence. Then, according to the well-known (k-ε)-turbulence model (see e.g. [1]), two more conservation equations for k and ε close the system. Note that for turbulent flows the standard (k-ε)-model is not valid near the solid surfaces where very strong velocity gradients occur. Therefore a special logarithmic law of the wall is used to simulate the turbulent boundary layer.

The Galerkin Weighted Residual Method is used to obtain a discrete model for the appropriately meshed flow region and a segregated algorithm is used to obtain a numerical solution of the problem. More detail information on the program can be found in [2].

At Pilatus Aircraft Ltd. CFD FLOTRAN (version 5.3) has been tested for its capability to perform turbulent flow calculation for the PC-9 trainer (Fig. 1) wing section.

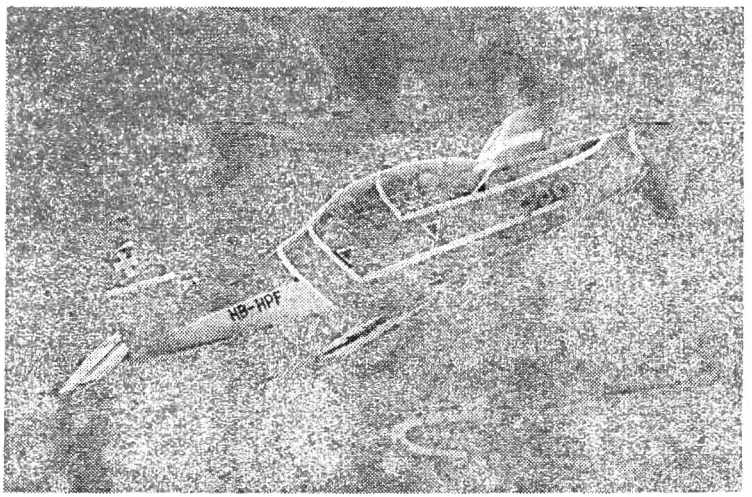

Fig. 1. PC-9 trainer

2. Transonic calculations

The following section is devoted to description and discussion of the results obtained for transonic calculation with the use of CFD FLOTRAN and comparison of the results with the results obtained by Daimler-Benz Aerospace and described in [3].

2.1. Initial data. The compressible transonic flow analysis for the PC-9 middle span wing section with the chord length c=1.652 m (the relative thickness t=0.13) is performed to simulate the cruise flight for the ISA standard day on the altitude 20000 ft with the airspeed 424 ktas. The angle of attack of the wing section α=1°. The flow is considered to be adiabatic, steady, viscous and compressible. The above altitude and velocity in FPS units correspond to 6096 m and v_∞=218.2 m/s in SI system. Therefore the parameters of the undisturbed air on this altitude for the ISA standard day (see e.g. [4]) are T=248.53 K, p=46.563 N/m^2, ρ=0.6527 kg/m^3. It is easy to check that the indicated values of T, P and ρ satisfy to the perfect gas law. Moreover, the sonic velocity a=316.03

m/s, kinematic viscosity $\nu=2.4383\cdot10^{-5}$ kg/s-m. This gives the Mach number $M=0.69$ and the Reynolds number $Re=14.7\cdot10^{6}$. The dimensionless parameters show that the flow under consideration is transonic and turbulent.

2.2. Mesh generation. Mesh generation is one of the most important steps of the finite element analysis. A CFD FLOTRAN macros is known for producing an O-mesh over 4-digit NACA airfoil series. In the present work the macros is generalized for the case of arbitrary airfoil. The input data for the macros is an ASCII file containing the number of points N and two columns of the airfoil coordinates XP and YP, starting from the trailing edge, along the upper surface and then along the lower surface. The point, corresponding to the trailing edge, appears twice – in the beginning and in the end of the coordinate table. The coordinates must also contain the point $x=0$, $y=0$ corresponding to the leading edge. The macros also contain parameters which allow to control the mesh density in different parts of the flow region. Its should be also noted that the macros is optimized to use minimal (independently of the number of the airfoil coordinates) number of keypoints, lines and areas. Therefore the macros can be applied even for educational versions of ANSYS.

For the given parameters of flow the thickness of the turbulent boundary layer on the airfoil can be estimated from the formula developed for turbulent incompressible flow past flat surface $\delta = 0.371c/\mathrm{Re}^{1/5} = 0.022$. Thus, the vertical resolution of the mesh near the airfoil surface must fine enough to contain several nodes within the indicated distance from the wall. Figure 2 shows a mesh produced near the airfoil which contain 16864 nodes. The size of the mesh is 10 times of the chord length. The maximal distance between the wall and the nearest node is 0.00099. The number of nodes on the upper and lowers surfaces is 115. General view on the mesh is presented in Fig. 3.

2.3. Boundary conditions and CFD FLOTRAN setup. The exterior nodes of the O-mesh are divided into the inlet nodes lying on the arc between $90+\alpha$ and $270+\alpha$ and the remaining outlet nodes. At the inlet nodes the velocity components $u=v_\infty\cos\alpha$, $v=v_\infty\sin\alpha$. Turbulent flow has a turbulence intensity level depending on the upstream conditions. The inlet turbulence level of a real flow is generally not known therefore some approximate values of k and ε should be found to obtain turbulence similar to the real flow. The inlet value of k can be evaluated approximately from the averaged inlet turbulence level of

wind tunnels. Usually $k \approx 0.05 \div 0.1$. The inlet value of ε then is calculated from $\varepsilon = C_\mu \rho k^2 / 0.01\mu$, i.e. under assumption that the inlet turbulent viscosity is $\mu_t = 0.01\mu$. In the case after consideration we put $k=0.0709$ what gives $\varepsilon=1855$.

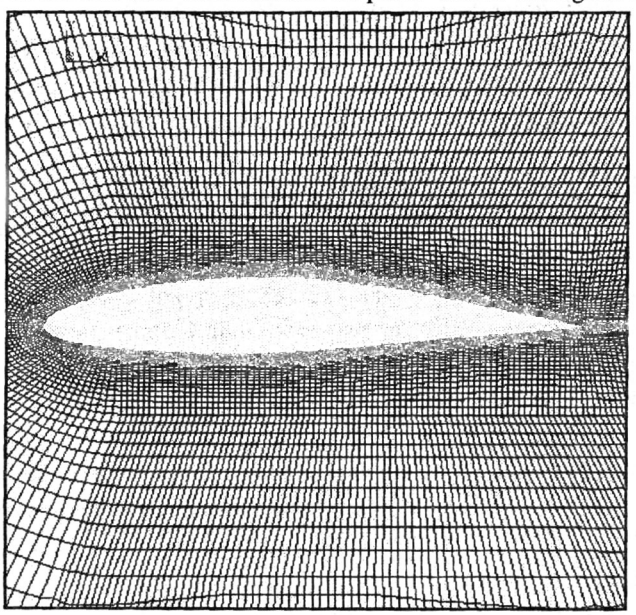

Fig. 2. Mesh generated over the airfoil.

In the outlet nodes only the pressure is prescribed. The program works with the relative pressure and the absolute pressure is obtained from the relative pressure by adding the reference pressure which in our case is 46563 Pa. Therefore in the outlet nodes which lies on the arc between $270+\alpha$ and $90+\alpha$ the relative pressure $p=0$. On the airfoil surface the non-slip conditions u=v=0 is used for all nodes.

The values $p=46563$ Pa, $T=248.53$ K, $\rho=0.6527$ kg/m^3 and $\nu=2.4383 \cdot 10^{-5}$ m^2/s where taken as reference values. The stability parameters for pressure and turbulence are set to 10^{-6}. The velocity capping is also using to avoid spurious values of velocity.

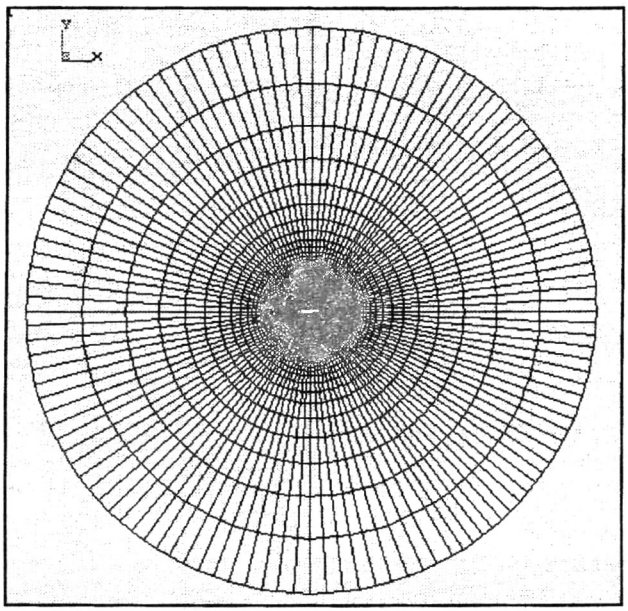

Fig. 3. General view on the mesh generated over the airfoil.

2.4. Results and discussion. Figure 4 shows constant Mach lines over the airfoil obtained for the mesh 1 after 2000 iterations. Convergence monitors for the pressure is $\approx 10^{-3}$, for the velocity components $\approx 10^{-5}$. The maximal Mach number on the airfoil is 1.465. On the upper surface one can clearly see a region with relatively more dense distribution of the constant Mach lines which corresponds to the transonic shock on the upper surface. Distribution of the negative pressure coefficient along the airfoil surface is presented in Fig. 5 with line 2. We see that around the middle

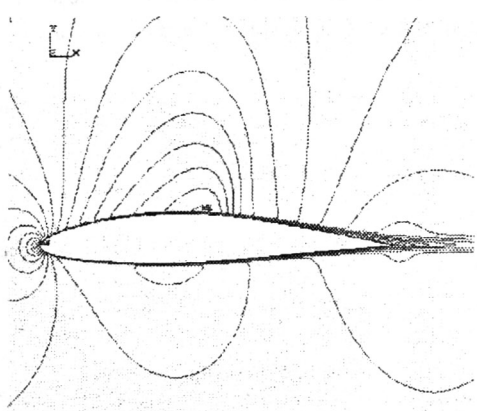

Fig. 4. Transonic calculation. Constant Mach lines.

chord of the airfoil the distribution is sharply decreasing. For comparison here we also present a negative pressure coefficient distribution (line 1) obtained for the same geometrical and aerodynamic data by an aerodynamic consultant contract to Pilatus [3] on a very fine mesh (65536 nodes) by solving the full Navier-Stokes equations. We see that comparing to these results the obtained distribution of the negative pressure coefficient has lower maximal value and the drop of the pressure is not so sharp. At the same time there is very good correspondence of the pressure coefficient distributions along the lower surface.

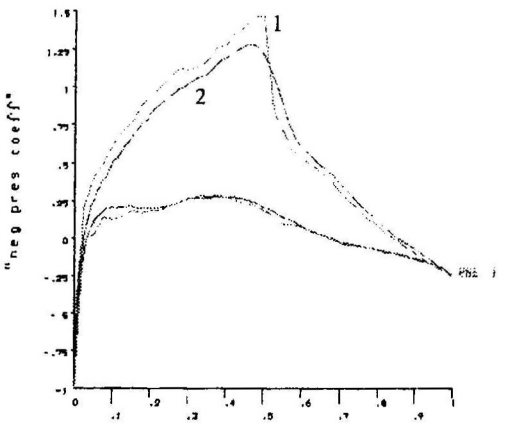

Fig. 5. Comparison of the pressure coefficient distributions. Line 1 – the results previously obtained by external consultant, line 2 – the present results.

Figure 6 shows comparison of the shear stress coefficients obtained with the use of CFD FLOTRAN (line 2) and from [3] (line 1). We see that distributions from [3] are decreasing near the leading edge what corresponds to the laminar part of the flow. Results obtained from CFD FLOTRAN have not laminar parts because, in the present simulation, turbulent flow is computed in the whole domain. That is why higher values of the shear stress coefficient are obtained near the leading edge. However this difference is negligi-

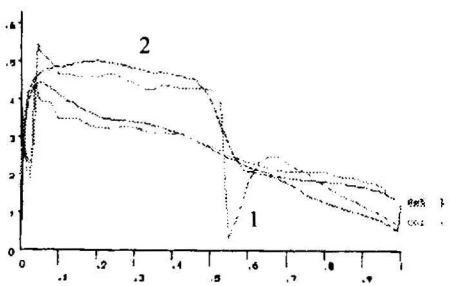

Fig. 6. Comparison of the wall shear stress coefficients distribution. Line 1 – the results previously obtained by external consultant, line 2 – the present results.

ble in computation of the forces acting on the airfoil. Past the transition point we see a very good correspondence of the shear stress coefficients on the lower surface. Along the upper surface the correspondence is rather good before the shock. After the shock both curves decrease sharply what corresponds to the boundary layer separation due to the high adverse pressure gradient. However according to [3] the drop is much deeper. After the shock the shear stress coefficient from [3] is recovered what corresponds to the reattachment of the boundary layer. According to the CFD FLOTRAN the separation flow does not reattach. This can be clearly seen in Fig. 7 where a zoom of the region near the shock is presented.

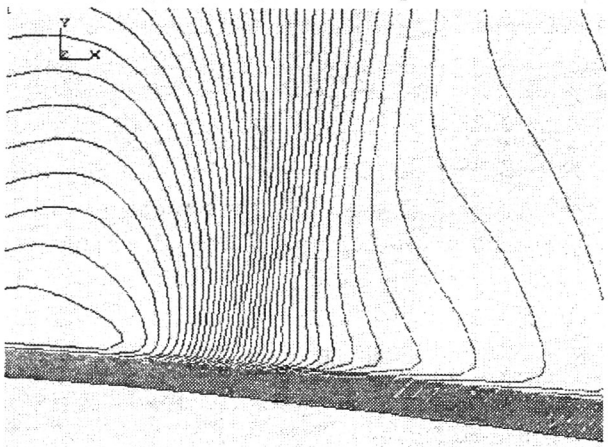

Fig. 7. Constant Mach lines near the shock position. Boundary layer separation due to the shock

The values of the force and the moment coefficients obtained with the use of CFD FLOTRAN are C_l=0.4805, C_d=0.0170, C_m=-0.0843. For comparison, in [3] C_l=0.5218, C_d=0.0120, C_m=-0.076. We see that the lift coefficient is lower, comparing to [3], due to the higher values of the maximal negative pressure coefficient on the upper surface. The values of the drag are higher and the moment coefficients are lower.

This and another calculations have shown that CFD FLOTRAN allows to obtain good results even on a rather coarse mesh. Particularly a good correspondence with results of [3] for the pressure distribution is obtained. For the shear stress coefficient, good coincidence is obtained for the turbulent part of the airfoil on the lower surface and on the upper surface before the shock. The difference in the lift coefficient comparing to [3] is 3-10%, the difference in the moment coefficient is 3-18%.

3. SUBSONIC STEADY STATE CALCULATIONS OF THE FLOW OVER AN AIRFOIL WITH A SPOILER

The following section is devoted to description and discussion of the results obtained with the use of CFD FLOTRAN for a steady subsonic flow over an airfoil with a spoiler and a pocket.

3.1. Initial data. Spoilers are aerodynamic devices that cause the flow to separate, resulting in loss of lift and increase in drag. Figure 8 shows a design of PC-9 middle span wing section with a spoiler and a pocket where the spoiler is placed before actuation. The length of the airfoil chord is c=1.725 m. The spoiler is placed on the distance of approximately 70% of the chord length from the leading edge. The angle between the spoiler and the airfoil surface is 60° that corresponds to the maximal deflection. The gap between the airfoil surface and the spoiler is approximately 10% of the spoiler chord. The operating conditions under which the spoiler is supposed to be used are: the velocity v_∞=123 m/s, α=0°, atmospheric conditions – the ISA standard day, sea level. This gives (see [4]) T=288.15 K, p=101325 Pa and ρ=1.225 kg/m^3. It is easy to check that the indicated values of T, P and ρ satisfy to the perfect gas law. Moreover, the sonic velocity a=340.29 m/s, kinematic viscosity ν=1.4607·10^{-5} kg/s-m. This gives the Mach number M=0.36 and Reynolds number Re=14.5·10^6. The flow parameters show that the flow under consideration is subsonic and turbulent and must have strongly separated character due to the presence of the spoiler and the spoiler pocket.

Fig. 8. Airfoil with spoiler and spoiler pocket.

3.2. Mesh generation. As it is noted already, generation of the mesh is one of the most important steps of the finite element analysis. In the previous Section a macros for producing mesh over a conventional airfoil is described. The same macros are used to produce an initial mesh over the airfoil with a spoiler. On the first step a mesh is generated over the isolated airfoil. Then the

area above the upper surface of the airfoil is cleared from the mesh and is subdivided into several subareas taking account for the geometry of spoiler and the spoiler pocket. Then each of these sub areas is meshed uniformly.

Figure 9 gives a detailed view onto the mesh near the spoiler with the presence of a pocket. As it is noted before, the meshing procedure involves uniform mesh generation in several sub areas near the spoiler. This can be seen in the figure. The main problem here is to obtain a smooth transition of the element size and shape through the boundary of the domains and at the same time to provide a more dense mesh near the spoiler edges and surface. The total number of nodes is 41151, the number of elements is 40864. The number of nodes on the airfoil surface including the pocket is 408, on the spoiler – 44.

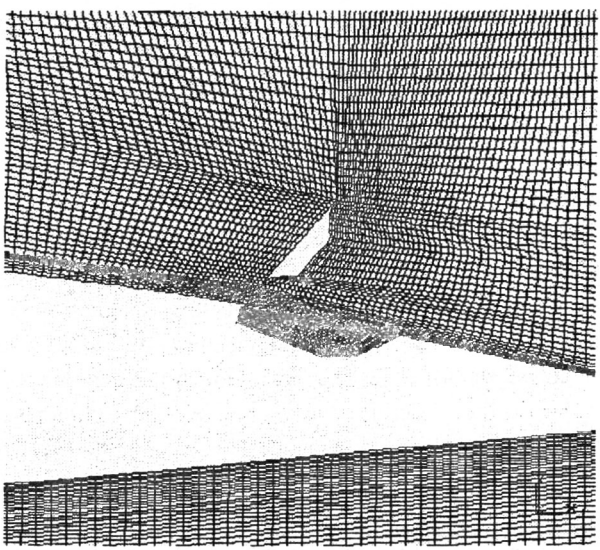

Fig. 9. Mesh near airfoil+spoiler+pocket.

3.3. Boundary conditions and FLOTRAN© setup. The way of prescribing the boundary conditions is already considered in 2.3. The exterior nodes are divided into the inlet nodes lying on the arc between $90°+\alpha$ and $270°+\alpha$ and the remaining outlet nodes. At the inlet nodes the velocity components $u=v_\infty\cos\alpha$, $v=v_\infty\sin\alpha$. A turbulent flow has a turbulence intensity level depending on the upstream conditions. The inlet turbulence level of a real flow is generally not known, therefore some approximate values of k and ε should be found to obtain turbulence similar to the real flow. The turbulent inlet values k and ε are also specified in the inlet nodes. The inlet value of k can be evaluated approximately from the averaged inlet turbulence level of wind tunnels. Usu-

ally $k \approx 0.05 \div 0.1$. The inlet value of ε then is calculated from $\varepsilon = C_\mu \rho k^2 / 0.01\mu$, i.e. under assumption that the inlet turbulent viscosity is $\mu_t = 0.01\mu$.

In the case under consideration it is taken $k=0.0709$, $\varepsilon=3097$. In the outlet nodes zero values of the relative pressure is prescribed. On the airfoil and the spoiler surfaces the non-slip conditions $u=v=0$ is used for all nodes.

The values $p=101325$ Pa, $T=288.15$ K, $\rho=1.225$ kg/m^3 and $\nu=1.4607 \cdot 10^{-5}$ m^2/s-m are taken as reference values. The stability parameters for pressure and turbulence are set to 1e-6. The velocity capping is also using to avoid spurious values of velocity.

3.4. Results and discussion. The following example is calculation of the steady subsonic flow over airfoil with spoiler and spoiler pocket. Figure 10 show constant velocity lines and streamlines for the solution obtained after 2000 iterations. The pressure convergence monitor is 10^{-3}, the velocity convergence monitor is 10^{-4}. One can see a small stagnation zone before the spoiler and jets separating from the spoiler upper and lower edges. However, due to the pocket the lower jet decelerates much faster now what brings more irregularity into the velocity picture. The maximal value of velocity is achieved on the lower edge of the spoiler and is equal to 249 m/s. There are two big vortexes right behind the spoiler and other near the trailing edge. One more vortex appears inside the pocket. The vortex picture can be more clearly seen in the picture presenting the flow streamlines. The value of the lift acting onto the airfoil is -5408 N per meter of span. The value of the drag force is 1847 N per meter of span. For the above reference data this corresponds to $C_l=-0.33$, $C_d=0.11$. This is close to the lift coefficient -0.5 predicted by the engineering data [6].

4. SUBSONIC TRANSIENT CALCULATIONS OF THE FLOW OVER AN AIRFOIL WITH A SPOILER

The transient numerical analysis is performed for separated flow over airfoil with a spoiler. An unsteady solution of the problem is obtained and discussed.

4.1. Set up the transient analysis. Numerical solutions for the airfoil with the spoiler obtained in the previous section show evident separation character of the flow past the spoiler. However separated flows are usually unsteady. Structure of the separated flow past airfoil periodically changes due to vortexes

periodically separating from the edges. Therefore the solution obtained in the previous section can be considered as time averaged solution and unsteady analysis is required to obtain more accurate results.

We perform unsteady analysis with the use of CFD FLOTRAN transient option. An important point of the unsteady analysis is the proper choice of the time step. For example, if c is the chord length, v_∞ – free stream velocity, *nelem* – number of elements along the chord, then the characteristic time required for a particle to pass the airfoil is $tchar=c/v_\infty$. and the time step is $tstep=tchar/nelem$. The minimal recommended number of the time steps is $ntime=2tchar/tstep$. For the present mesh around the airfoil with the spoiler and pocket have $tstep=10^{-5}$. CFD FLOTRAN allows an automatic time step choice that is based on the above reasoning and moreover involves some convergence control. Below we use the automatic time step choice option.

We take the steady state solution obtained in the previous section (Fig. 10) as initial for the transient analysis. The pressure and the velocity convergence monitors for this solutions are small enough, therefore we perform only one global iteration per time step.

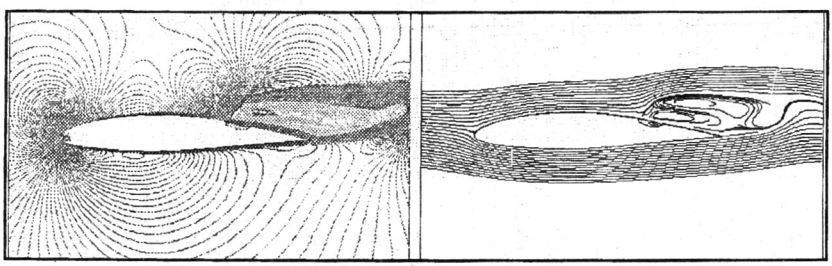

Fig.10. Frame 1. Stationary solution. The vortex just separated from the trailing edge.

4.2. Results and discussion. To monitor the convergence of the transient analysis we use the value of the loads on the spoiler and on the airfoil. After 20000 iterations the forces has stabilized more or less at the total lift – -8258 N per meter of span (C_l=-0.52), the total drag – 1847 N per meter of span (C_d=0.12), the normal load onto the spoiler – -1441 N per meter of the span. For t>0.07 the values of the loads does not change much with the time. Nevertheless the flow is periodical. Every 0.016 a vortex is separated from the trailing edge of the airfoil. This corresponds to the frequency 64 Hz. Figures 10-14

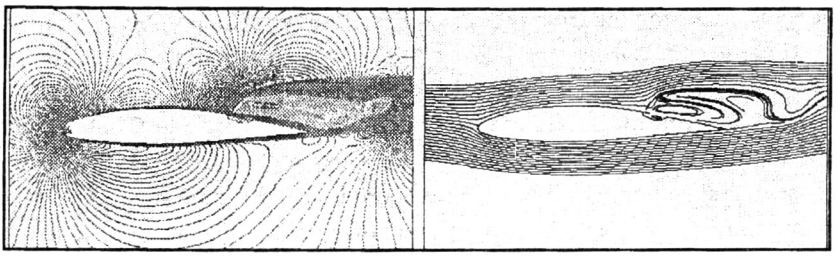

Fig. 11. Frame 2. The vortex starts to travel upstream.

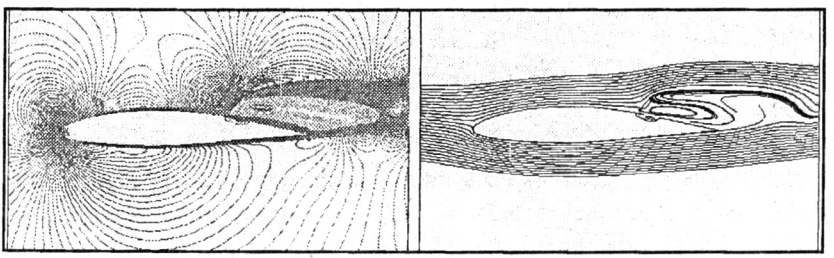

Fig. 12. Frame 4. The vortex has gone away.
The next vortex is about to appear near the trailing edge.

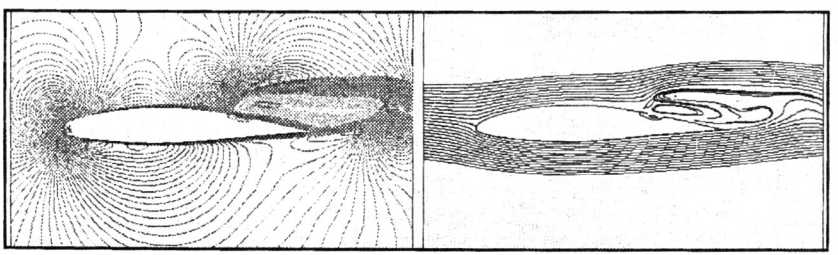

Fig. 13. A new vortex appeared on the trailing edge.

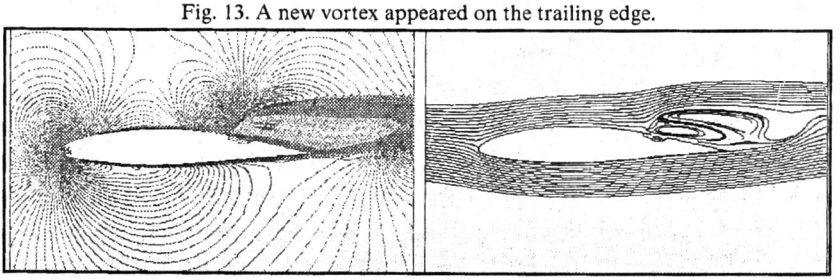

Fig. 14. The vortex has separated from the trailing edge.

show the time sequence of 5 frames containing constant velocity lines and streamlines within one period. We see here two big stable vortexes behind the spoiler turning in the opposite direction. A small vortex is inside the spoiler pocket. Another vortex is periodically separating from the trailing edge of the airfoil. In the first frame (Fig. 10) we see the vortex which has just separated from the trailing edge. In the second frame (Fig. 11) the vortex starts to travel upstream. In the frame 3 (Fig. 12) we see the beginning of a new vortex generation near the trailing edge of the airfoil. The vortex is generated and is about to separate from the trailing edge in the frame 4 (Fig. 13). The frame 5 (Fig. 14) shows a new vortex, which has just separated from the trailing edge.

References

1. Launder B.E., Spalding D.B. The numerical computation of turbulent flows. Computer methods in 2.CFD FLOTRAN. Analysis Guide. Release 5.3. SAS IP, Houston, 1996.
2. Numerical investigation of transonic aerodynamic characteristics of the PILATUS PC-9 trainer aircraft. Contractor Report by external consultant using a full Navier Stockes code.
3. Engineering Science Data Unit, Item Number 77021. ESDU Ltd., London, 1973.
4. Applied Mechanics and Engineering, 1974, V. 3, P. 269–289.
5. Engineering Science Data Unit, Item Number 90030. ESDU Ltd., London, 1973.
6. Internal Pilatus report on the investigations of the use of spoilers (utilizes [5])